EPSC Abstracts
Vol. 12, EPSC2018-1091, 2018
European Planetary Science Congress 2018

Far-IR Emissivity in Lunar South Polar Permanently Shaded Terrain: Apparent Temperature Dependence

Elliot Sefton-Nash (1), Jean-Pierre Williams (2), Joshua Bandfield (3), Tristram Warren (4), Benjamin T. Greenhagen (5) and, David A. Paige (2).
(1) ESTEC, European Space Agency, Keplerlaan 1, Noordwijk 2201AZ, Netherlands (e.sefton-nash@cosmos.esa.int) (2) Department of Earth, Planetary and Space Sciences, University of California Los Angeles, CA, USA. (3) Space Science Institute, Boulder, CO, USA. (4) Department of Physics, University of Oxford, UK. (5) Applied Physics Laboratory, Johns Hopkins University, Baltimore, MD, USA.

1. Introduction

The northern floor and wall of Amundsen crater, near the lunar south pole, is a permanently shadowed region. We report on interpretation of results from observations of two targets on the floor of Amundsen, one in the permanently shadowed region (PSR) and the other in the partially illuminated area (NPSR) (Figure 1), with the goal of observing relative differences in their far-IR emissivity in nighttime observations by LROs Diviner Lunar Radiometer Experiment. A 3km radius around centers of 93.1047°E, 84.5523°S and 91.2826°E, 83.6889°S define the NPSR and PSR targets, respectively.

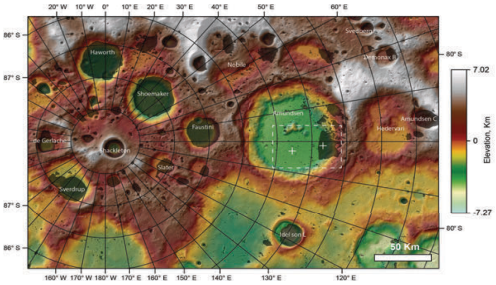

Figure 1: Study area and targets: colorized hillshade from LOLA 20m/pix data. Regions in permanent shadow darkened using 120 m/pixel map [1]. Dashed box contains 2 targets in Amundsen crater marked with white '+'s.

The permanently shadowed target includes terrain that is reported to indicate generally brighter 1064 nm albedo combined with annual maximum surface temperatures low enough to enable persistence of surface water ice (< 110K). Many permanently shadowed areas with similar LOLA reflectance characteristics do not show this trend [2].

This is consistent with a similar correlation of annual maximum temperature with anomalous ultraviolet radiation as measured by the LAMP instrument [3]. A patchy distribution of areas in the PSR target show a combination of off/on-band ratios > 1.2 and Lyman-α albedo < 0.03, indicating a possible water mass content of 0.1 – 2.0% [4].
Portions of our PSR target therefore indicate annual maximum temperatures, as well as ultraviolet and near-IR signatures that are anomalous compared to other south polar terrain in permanent shadow, consistent with the presence of surface water frost.

Indeed, our intent in previous work was to determine if the presence of water frost could be verified through study of far-IR emissivity trends, near the planck peak at PSR temperatures.

2. Method

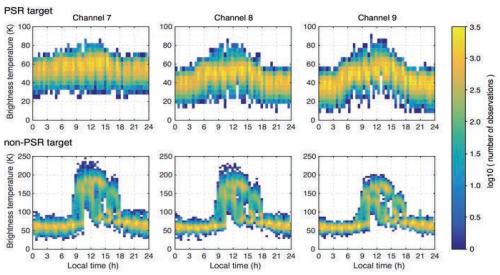

Figure 2: Brightness temperatures observed for PSR (top) and NPSR (bottom) targets between Jul. 2009 – Aug. 2017) plot over local mean solar time (LMST).

To quantify deviations in observed emissivity from what would be expected from planck emission, we model the band ratio of channels 8 and 9 ($\Re_{8/9}$) as a function of surface temperature, because these long wavelength channels are most sensitive to PSR-relevant temperatures. This model allows us to plot the tentative signature of changes in apparent emissivity as a function of surface temperature, without assuming a value for emissivity.
After differencing the model with observations as a function of bolometric brightness temperature (T_{BOL}: the channel-integrated best estimate of surface kinetic temperature), we previously asserted that the offset in $\Re_{8/9} - \Re_{8/9model}$ for the PSR target and its apparent temperature dependence at temperatures < 40 K, may indicate different thermophysical gradients between

the targets, perhaps attributed to surface layers, including surface water frost.

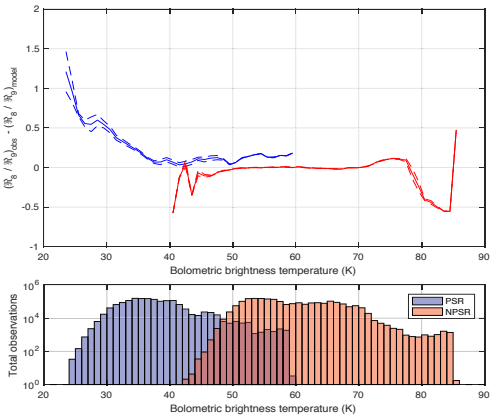

Figure 3: Band ratio model vs observations ±1σ over T_{BOL}.

3. Discussion

Here we update our interpretation of these results to consider the possible effects of surface roughness in PSRs. Sub-field of view (FOV) scale "micro" doubly-shadowed cold traps, topographic lows in PSRs that are also protected from secondary and higher order thermal emission (e.g. from crater walls), may contribute to anisothermality in PSRs. We construct a simple model that considers radiance contributions from a bi-modal brightness temperature distribution (Figure 4). PSR terrain is fixed at 40K, and $\mathfrak{R}_{8/9}$ is modelled as the temperature, and fraction, of doubley-shadowed PSRs is varied. Figure 4 shows the deviation of $\mathfrak{R}_{8/9}$ over these parameters from that expected from a homogenous temperature distribution at 40K. Deviation is largest when PSR and double PSR are similar in temperature (and therefore signal), but also when temperature hetereogeneity is largest. For PSR material at 40K (typical for nighttime PSR temperatures, Fig. 2), low to modest fractions (0-0.6) of micro cold traps, that are just a few K cooler than the PSR terrain, could produce the observed deviation in $\mathfrak{R}_{8/9} - \mathfrak{R}_{8/9model}$.

Apparent temperature dependence could also be explained by this mechanism, simply because there are many observations and their FOV contents do not all have the same micro double-PSR fraction.

The range of different micro-cold trap fractions in FOVs leads to a range of brightness temperatures, and degrees of ansiothermality. Colder brightness temperatures may result from larger fractions of, or colder, doubley shadowed regions within an FOV.

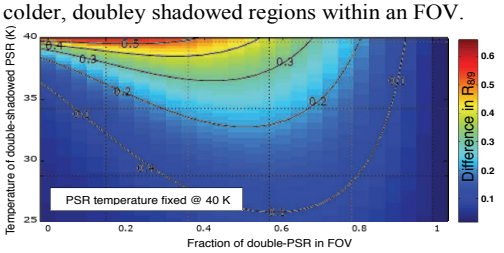

Figure 4: Magnitude of difference in $\mathfrak{R}_{8/9}$ between bi-modal and unimodal temperature distribution in a FOV on a PSR. PSR temperature fixed at 40K, and fraction of double-shadowed PSR, and its T, are varied.

4. Conclusions

The nighttime radiance ratio between Diviner channels 8 and 9, distinguishes a PSR from a non-PSR target on the floor of Amundsen crater in two ways: 1) Data for the PSR target is always positively offset from the non-PSR target, indicating that emission in channel 9 decreases relative to that in 8. 2) The effect becomes temperature dependant < 40 K, and increases with decreasing temperature. Building on previous results, we interpret that there may be two possible causes: **1)** The two targets may have different gradients in thermophysical properties due to different epiregolith structure [e.g. Mendell and Noble, 2010], possibly including surface water frost suggested in other studies. Such structure may be responsible for temperature dependant thermal conductivity [e.g. 7, 8]. **2)** The offset and temperature-dependent anisothermality for the PSR target may be attributed to sub-EFOV scale "micro" cold traps that are not resolved in the Diviner data. Using a simple model, and depending on the fraction of cold-traps in a given EFOV, these micro cold traps could be a few to several 10s of degrees K colder than the surrounding PSR.

References

[1] Marzarico et al., (2011), Icarus 211, p. 1066-1081. [2] Fisher, E. A. et al. (2017), *Icarus* 292, p. 74-85. [3] Gladstone, G. R. et al. (2012), *J. Geo. Res.* 117, E00H04. [4] Hayne, P. O. et al. (2015), Icarus 255, p. 58-69. [5] Williams, J.-P. et al., (2016), Icarus 273, p. 205-213. [6] Paige D. A. et al. (2010), Space Sci. Rev. 150, p. 125–160. [7] Woods-Robinson, R. et al. (2016) AGU, Abs. P21A-2077. [8] Siegler, M. A. et al. (2016) AGU, Abs. P24A-05.